

# Swi3p controls SWI/SNF assembly and ATP-dependent H2A-H2B displacement

Xiaofang Yang<sup>1</sup>, Roser Zaurin<sup>2</sup>, Miguel Beato<sup>2</sup> & Craig L Peterson<sup>1</sup>

**Yeast SWI/SNF is a multisubunit, 1.14-MDa ATP-dependent chromatin-remodeling enzyme required for transcription of a subset of inducible genes. Biochemical studies have demonstrated that SWI/SNF uses the energy from ATP hydrolysis to generate superhelical torsion, mobilize mononucleosomes, enhance the accessibility of nucleosomal DNA and remove H2A-H2B dimers from mononucleosomes. Here we describe the ATP-dependent activities of a SWI/SNF subcomplex that is composed of only three subunits, Swi2p, Arp7p and Arp9p. Whereas this subcomplex is fully functional in most remodeling assays, Swi2p-Arp7p-Arp9p is defective for ATP-dependent removal of H2A-H2B dimers. We identify the acidic N terminus of the Swi3p subunit as a novel H2A-H2B-binding domain required for ATP-dependent dimer loss. Our data indicate that H2A-H2B dimer loss is not an obligatory consequence of ATP-dependent DNA translocation, and furthermore they suggest that SWI/SNF is composed of at least four interdependent modules.**

The assembly of eukaryotic DNA into folded nucleosomal arrays is likely to have a major impact on the efficiency or regulation of nuclear processes that require access to the DNA sequence, including RNA transcription, DNA replication, recombination and repair. In fact, it is now generally recognized that disruption or remodeling of chromatin structure may be a prerequisite step for most of these nuclear DNA transactions. Two classes of highly conserved chromatin remodeling and modification enzymes have been implicated as regulators of the repressive nature of chromatin structure. The first class includes enzymes that covalently modify the nucleosomal histones (by acetylation, phosphorylation, methylation, ubiquitination and so forth)<sup>1,2</sup>, and the second class is composed of multisubunit complexes that use the energy of ATP hydrolysis to disrupt histone-DNA interactions<sup>3</sup>.

The *Saccharomyces cerevisiae* SWI/SNF complex is a prototype for ATP-dependent chromatin-remodeling enzymes. Yeast SWI/SNF is a multisubunit complex that consists of Swi2p (also called Snf2p), Swi1p, Snf5p, Swi3p, Swp82p, Swp73p, Arp7p, Arp9p, Snf6p, Snf11p and Swp29p, with a molecular weight of 1.14 MDa<sup>4-9</sup>. This widely conserved assembly is required for the inducible expression of a number of diversely regulated yeast genes and for the full functioning of many transcriptional activators<sup>10</sup>. SWI/SNF can be recruited to target genes through direct interactions with gene-specific activators, and in several cases SWI/SNF facilitates the binding of activators to nucleosomal sites *in vivo*<sup>11-14</sup>. *In vitro*, the purified SWI/SNF complex is a DNA-stimulated ATPase that can use the energy from ATP hydrolysis to disrupt histone-DNA interactions. Although the precise mechanism of SWI/SNF action is not clear, recent studies, including single-molecule studies, have suggested a model in which SWI/SNF

uses a DNA 'pumping' mechanism to generate transient DNA loops on the histone octamer surface<sup>15-17</sup>. This ATP-dependent DNA translocation model is consistent with the ability of SWI/SNF to use the energy of ATP hydrolysis to generate superhelical torsion, mobilize nucleosomes and enhance nucleosomal DNA accessibility<sup>3</sup>. SWI/SNF remodeling can also lead to the removal of one or both histone H2A-H2B dimers from a mononucleosome substrate, and this reaction is sensitive to the underlying sequence of nucleosomal DNA<sup>18,19</sup>. Whether this dimer-loss reaction is simply an indirect consequence of the DNA-translocation reaction is not known.

The catalytic subunit of yeast SWI/SNF is Swi2p/Snf2p, which is the founding member of a subfamily of the SF2 superfamily of DNA-stimulated ATPases and helicases<sup>20</sup>. A human homolog of Swi2p/Snf2p, BRG1, is the catalytic subunit of the human SWI/SNF complex, and the isolated BRG1 subunit is able to alter histone-DNA interactions on a mononucleosome substrate<sup>21,22</sup>. If the ATPase subunit is sufficient for ATP-dependent remodeling, what are the role(s) of the other subunits? Two subunits, Swi1p and Snf5p, interact with the acidic activation domains of gene-specific activators, and these interactions are essential for recruitment of SWI/SNF to target loci<sup>11</sup>. Early studies demonstrated that at least four subunits of SWI/SNF (Swi1p, Swi3p, Snf5p and Snf6p) are required for assembly of the Swi2p/Snf2p subunit into a high-molecular weight complex, and inactivation of these subunits leads to phenotypes identical to those of a *swi2* mutant<sup>5,23</sup>. In contrast, the Swp82p<sup>24</sup>, Swp29p<sup>7</sup> and Snf11p subunits do not seem to be essential for SWI/SNF function *in vivo*<sup>8</sup>.

The Swi3p subunit of SWI/SNF contains a conserved SANT domain. This domain functions as a histone N-terminal tail-interaction

<sup>1</sup>Interdisciplinary Graduate Program, Program in Molecular Medicine, University of Massachusetts Medical School, Worcester, Massachusetts 01605, USA. <sup>2</sup>Centre de Regulació Genòmica, Universitat Pompeu Fabra, PRBB, Dr. Aiguader 88, E-08003 Barcelona, Spain. Correspondence should be addressed to C.L.P. (craig.peterson@umassmed.edu).

Received 5 December 2006; accepted 23 March 2007; published online 13 May 2007; doi:10.1038/nsmb1238

module in yeast Ada2p<sup>25</sup>, a subunit of multiple histone acetyltransferase complexes<sup>26</sup>. Previously, we have demonstrated that an 11-amino acid residue deletion within the Swi3p SANT domain (*swi3-ΔSANT*) yields *swi* or *snf* mutant phenotypes, suggesting that this domain is key in SWI/SNF function<sup>25</sup>. Here we investigate the role of the Swi3p SANT domain in SWI/SNF function. We describe the purification of SWI/SNF from the *swi3-ΔSANT* strain, and we show that this small deletion leads to the dissociation of SWI/SNF into at least four subcomplexes: (i) Swi2p–Arp7p–Arp9p, (ii) Swi3p–Swp73p–Snf6p, (iii) Snf5p and (iv) Swi1p. Purification of SWI/SNF from strains that lack the entire Swi3p, Snf5p or Swi1p subunit supports the view that these four subcomplexes define a modular organization of SWI/SNF. Characterization of the Swi2p–Arp7p–Arp9p subcomplex demonstrates that it has ATPase and chromatin-remodeling activities that are equivalent to those of intact SWI/SNF. The one exception, however, is that the Swi2p–Arp7p–Arp9p subcomplex is defective in catalyzing histone H2A–H2B dimer loss. We show that dimer loss requires an acidic N-terminal domain of the Swi3p subunit, which binds specifically to the N-terminal domains of histones H2A and H2B *in vitro*. These data indicate that the Swi3p subunit provides a histone-chaperone function that is essential for efficient removal of histone H2A–H2B dimers during ATP-dependent remodeling.

## RESULTS

### The Swi3p SANT domain is required for SWI/SNF assembly

The SANT domain was originally identified as a ~50-residue module related to the c-Myb DNA-binding domain<sup>27</sup>. Recent studies have demonstrated that the SANT domains found in Ada2p, Rsc8p and Swi3p are essential for the functioning of Gcn5p-containing HAT complexes, the RSC and SWI/SNF ATP-dependent remodeling complexes, respectively<sup>25,28</sup>. In the case of Ada2p, the SANT domain is key in functional and physical interactions with the histone H3 N-terminal tail<sup>25</sup>. Likewise, the SANT domain in the mammalian nuclear hormone receptor corepressor SMRT is also involved in coordinating histone deacetylase HDAC3 activity with histone tail interactions<sup>29</sup>. These studies have led to the view that the SANT domain is a previously uncharacterized type of histone tail–interaction domain<sup>30</sup>.

To further characterize the role of the essential SANT domain in Swi3p, we used a tandem affinity purification (TAP) method to purify SWI/SNF complex from wild-type and *swi3Δ* strains, and from a *swi3-ΔSANT* strain, which harbors an 11-residue deletion within the SANT domain. Consistent with our previous studies<sup>4</sup>, purification of the TAP-tagged Swi2p subunit from a wild-type strain yielded a SWI/SNF complex composed of 11 subunits, although the small subunits, Snf1p and Swp29p, were not stained well by silver (Fig. 1a, lane 1). Complete removal of the Swi3p subunit (data not shown) or a small deletion within the Swi3p SANT domain led to disassembly of the SWI/SNF complex, as only the Arp7p and Arp9p subunits copurified with Swi2p (Fig. 1a, lane 2). The abundance of a large polypeptide was variable among Swi3p–ΔSANT preparations, and mass spectrometry indicated that this species is a proteolytic product of Swi2p (data not shown). Identical results were found when

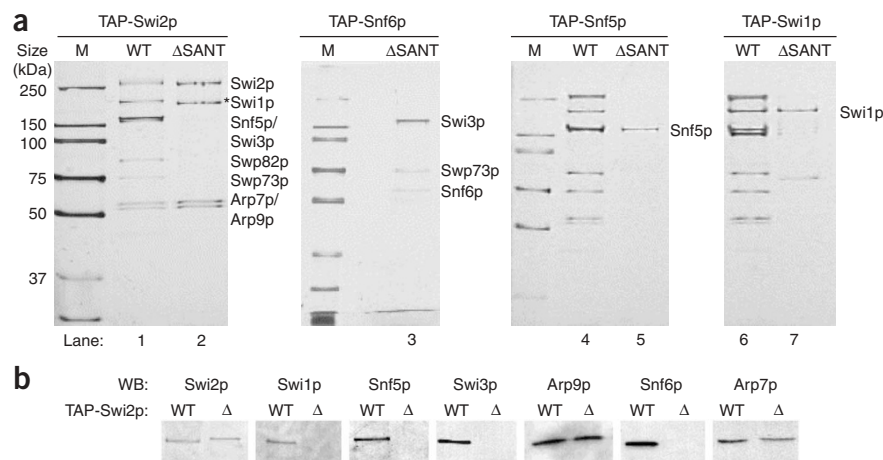


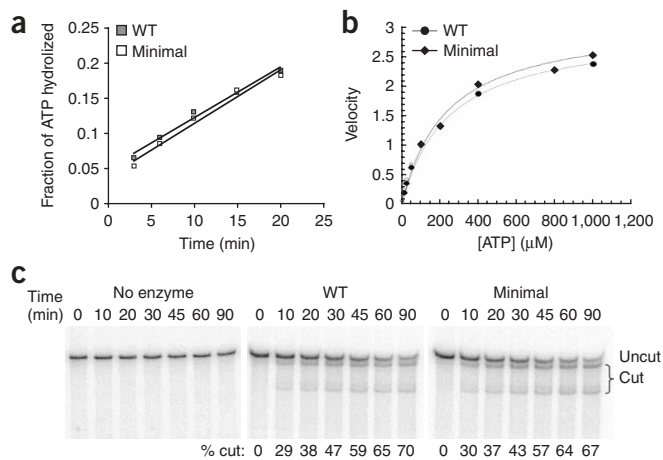
**Figure 1** The SANT domain of Swi3p is required for SWI/SNF assembly. (a) TAP-Swi2p, TAP-Snf6p, TAP-Snf5p and TAP-Swi1p proteins were purified from wild-type (WT) or *swi3-ΔSANT* (ΔSANT) strains. Approximately one-tenth of each preparation was resolved on 8%–10% SDS PAGE for silver staining. M, molecular weight marker. Asterisk in lane 2 represents breakdown product of Swi2p. (b) Western blots of TAP-Swi2p preparations purified from WT or *swi3-ΔSANT* strains using polyclonal antibodies specific for each of the indicated subunits.

SWI/SNF was purified from a *swi3* mutant carrying a single-amino acid change within the Swi3p SANT domain (Swi3-R564E; data not shown). Consistent with a role for the SANT domain in SWI/SNF assembly, the 11-residue deletion in the Swi3p SANT domain also altered the elution of Swi2p when whole-cell extracts were fractionated on a Superose 6 gel-filtration column (data not shown). Changes in the SANT domain do not affect Swi3p expression<sup>25</sup>; thus, Swi3p and an intact Swi3p SANT domain are required for the assembly of an intact SWI/SNF complex.

To trace the missing components of SWI/SNF, we generated alleles encoding TAP-tagged Snf6p, Swi1p and Snf5p in both wild-type and *swi3-ΔSANT* strain backgrounds. Tandem affinity purifications of these tagged subunits from a wild-type strain repeatedly led to the purification of an intact SWI/SNF complex (Fig. 1a, lanes 4 and 6, and data not shown). In contrast, when these subunits were purified from the *swi3-ΔSANT* strain, TAP-Snf6p copurified with only the Swi3p and Swp73p subunits (Fig. 1a, lane 3), and TAP-Snf5p and TAP-Swi1p appeared to purify as single polypeptides (Fig. 1a, lanes 5 and 7). Western blotting and mass spectrometry verified the subunit composition of each putative subcomplex (Fig. 1b and data not shown). We also purified TAP-Snf5p from a *swi2Δ* strain, TAP-Snf5p from a *swi1Δ* strain and TAP-Snf6p from a *snf5Δ* strain (data not shown). As expected from earlier studies<sup>5</sup>, each of these SWI or SNF subunit gene deletions led to disassembly of SWI/SNF (data not shown). All of the data are fully consistent with a structural organization of SWI/SNF that involves the interdependent assembly of four distinct subcomplexes: (i) Swi2p–Arp7p–Arp9p, (ii) Swi3p–Swp73p–Snf6p, (iii) Snf5p and (iv) Swi1p.

### The Swi2p subcomplex has ATP-dependent remodeling activity

We tested both DNA- and nucleosome-stimulated ATPase activity of each subcomplex that was purified from *swi3-ΔSANT* or *swi3Δ* strains. As might be expected, only the Swi2p–Arp7p–Arp9p subcomplex had detectable ATPase activity, and its DNA-stimulated (Fig. 2a) and nucleosome-stimulated ATPase activity (data not shown) were identical to that of intact SWI/SNF. We further investigated the kinetics of



ATP hydrolysis by the Swi2p-Arp7p-Arp9p subcomplex. The initial velocities of the ATPase reaction were determined at various ATP concentrations from the slopes of linear ATP hydrolysis plots. Velocities were plotted as a function of ATP substrate concentration and fit to the Michaelis-Menten equation. The kinetic parameters averaged from three independent experiments showed that intact SWI/SNF has a  $K_m$  of  $231.9 \pm 32.4 \mu\text{M}$  and a  $V_{max}$  of  $3.1 \pm 0.2 \mu\text{M min}^{-1}$ , and the Swi2p-Arp7p-Arp9p subcomplex has a  $K_m$  of  $242.6 \pm 47.6 \mu\text{M}$  and  $V_{max}$  of  $3.0 \pm 0.2 \mu\text{M min}^{-1}$  (Fig. 2b). These results further confirm that the ATPase activity of this minimal complex is identical to that of intact SWI/SNF.

### Swi2p subcomplex is an active chromatin-remodeling enzyme

As Swi2p-Arp7p-Arp9p has ATPase activity that is identical to that of intact SWI/SNF, we asked whether this subcomplex could couple ATP hydrolysis to chromatin remodeling. First, we tested whether the Swi2p-Arp7p-Arp9p subcomplex can generate superhelical torsion on a DNA substrate in an ATP-dependent reaction. A previous study has indicated that the generation of superhelical torsion is a basic feature of ATP-dependent chromatin-remodeling enzymes, and this activity is likely to reflect the ATP-dependent translocation of DNA<sup>31</sup>. In these assays, we used a linear, <sup>32</sup>P-labeled DNA template containing an inverted (A+T)-rich sequence that is extruded into a cruciform structure by ATP-dependent production of superhelical torsion by remodeling enzymes<sup>31</sup>. Formation of the cruciform can be detected by T4 endonuclease VII cleavage. Similar to previous results<sup>31,32</sup>, SWI/SNF was able to catalyze cruciform extrusion, as demonstrated by the time-dependent T4 endonuclease VII cleavage of the DNA into two small fragments (Fig. 2c). Likewise, equal amounts of the Swi2p-Arp7p-Arp9p subcomplex provided equivalent rates of ATP-dependent cruciform formation (Fig. 2c), suggesting that this subcomplex is fully functional in this DNA-based reaction.

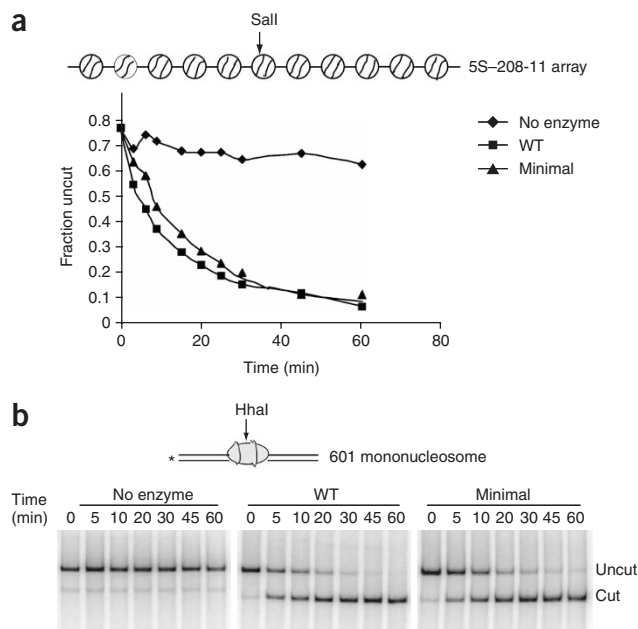
A hallmark of ATP-dependent remodeling enzymes is the ability to use the energy from ATP hydrolysis to increase restriction enzyme

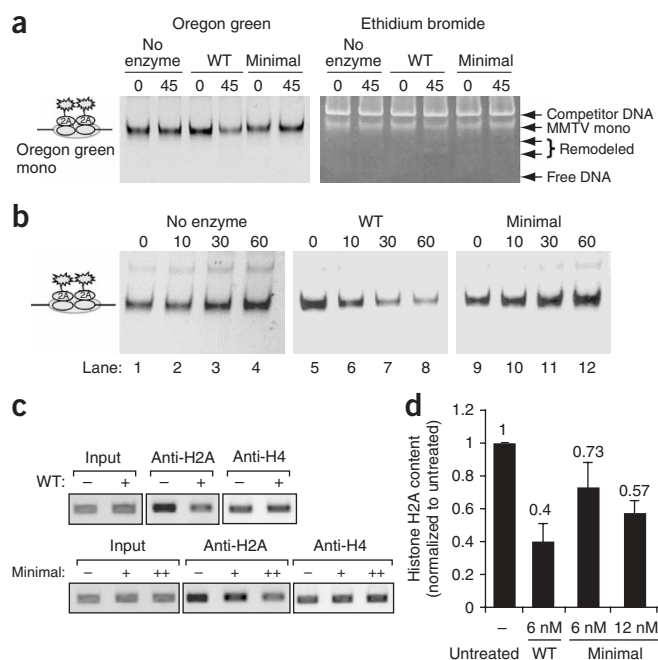
accessibility on mononucleosomes or nucleosomal arrays. To investigate the functioning of the Swi2p-Arp7p-Arp9p subcomplex in this type of assay, we used stepwise salt dialysis to reconstitute <sup>32</sup>P-labeled nucleosomal arrays with recombinant *Xenopus laevis* histone octamers and a DNA template that consists of 11 tandem repeats of a nucleosome-positioning sequence from 5S ribosomal DNA. In these arrays, the central nucleosome-positioning sequence contains a unique Sall restriction enzyme recognition site that is occluded by nucleosome assembly (Fig. 3a, top)<sup>33</sup>. In the presence of intact SWI/SNF and ATP, Sall digestion kinetics was greatly enhanced (Fig. 3a). The Swi2p-Arp7p-Arp9p subcomplex showed equivalent activity in this assay (Fig. 3a). Similar results were obtained when the remodeling enzymes were present in stoichiometric or substoichiometric amounts with respect to nucleosomes (data not shown).

Restriction enzyme-accessibility assays were also done with mononucleosome substrates. Mononucleosomes were reconstituted onto a <sup>32</sup>P-labeled 343-base-pair (bp) DNA fragment that harbored the 601 nucleosome-positioning sequence (Fig. 3b, top)<sup>34</sup>. A unique HhaI restriction enzyme site is occluded by nucleosome assembly and is located close to the nucleosomal dyad. In the absence of SWI/SNF, there was little HhaI digestion of the mononucleosomal substrate, whereas addition of SWI/SNF and ATP led to more than 90% cleavage of nucleosomal DNA by 60 min (Fig. 3b). Likewise, the Swi2p-Arp7p-Arp9p subcomplex showed equivalent activity in this assay (Fig. 3b).

Restriction enzyme-accessibility assays were also done with mononucleosome substrates. Mononucleosomes were reconstituted onto a <sup>32</sup>P-labeled 343-base-pair (bp) DNA fragment that harbored the 601 nucleosome-positioning sequence (Fig. 3b, top)<sup>34</sup>. A unique HhaI restriction enzyme site is occluded by nucleosome assembly and is located close to the nucleosomal dyad. In the absence of SWI/SNF, there was little HhaI digestion of the mononucleosomal substrate, whereas addition of SWI/SNF and ATP led to more than 90% cleavage of nucleosomal DNA by 60 min (Fig. 3b). Likewise, the Swi2p-Arp7p-Arp9p subcomplex showed equivalent activity in this assay (Fig. 3b).

**Figure 3** Chromatin-remodeling activity of the minimal Swi2p-Arp7p-Arp9p subcomplex. (a) Schematic of the 5S-208-11 nucleosomal array substrate. Reactions containing 1 nM of the wild-type SWI/SNF or the minimal Swi2p-Arp7p-Arp9p subcomplex were incubated with 2 nM nucleosomal array, 1 mM ATP and 10 units Sall restriction enzyme. (b) Schematic of 343-bp 601 mononucleosome substrate. Reactions containing 1 nM SWI/SNF or minimal Swi2p-Arp7p-Arp9p subcomplex were incubated with 2 nM 601 mononucleosome, 1 mM ATP and 10 units HhaI restriction enzyme.





One of the mechanisms by which SWI/SNF catalyzes chromatin remodeling is by mobilization of a histone octamer bidirectionally toward the ends of a DNA template<sup>35,36</sup>. These end-positioned nucleosomes migrate faster than the original, centrally positioned species during nondenaturing gel electrophoresis<sup>37</sup>. The 601 mononucleosome substrates were also used for nucleosome-mobilization assays (Supplementary Fig. 1 online). In this case, mononucleosomes were remodeled by SWI/SNF or the Swi2p-Arp7p-Arp9p subcomplex, the remodeling enzyme was removed by competition with unlabeled DNA, and then the nucleosome products were electrophoresed on a nondenaturing polyacrylamide gel. Both the intact and Swi2p-Arp7p-Arp9p subcomplexes were able to generate more quickly migrating mononucleosome species with similar kinetics (Supplementary Fig. 1). Together, these different approaches demonstrate that the Swi2-Arp7-Arp9 subcomplex is a robust chromatin-remodeling enzyme and that the other eight SWI/SNF subunits do not contribute appreciably to these remodeling activities.

### H2A-H2B displacement requires an intact SWI/SNF complex

Recent studies showed that SWI/SNF can catalyze the displacement of histone H2A-H2B dimers from a nucleosomal substrate<sup>18</sup>. Subsequently, it was shown that this dimer-displacement activity is sensitive to the underlying sequence of the nucleosomal substrate: SWI/SNF shows potent dimer-displacement activity with an MMTV mononucleosome<sup>19</sup> but no appreciable dimer-displacement activity with an rDNA substrate<sup>19</sup> or 601 mononucleosome<sup>36</sup>. Notably, SWI/SNF-dependent H2A-H2B dimer displacement seems to be key in the activation of the MMTV promoter *in vivo* by progesterone receptor<sup>19</sup>.

To quantify the efficiency of dimer displacement by intact and minimal SWI/SNF complexes, we used a strategy developed by Owen-Hughes and colleagues<sup>18</sup> in which MMTV mononucleosomes are reconstituted with recombinant histone octamers that harbor an Oregon green fluorescent group covalently coupled to a unique cysteine residue on the C-terminal tail of histone H2A (H2A-S113C). After electrophoresis on a 4% nondenaturing polyacrylamide gel, reconstituted MMTV mononucleosomes migrate to a single predominant position, as detected by Oregon green fluorescence

(Fig. 4a, left gel) and ethidium bromide staining (Fig. 4a, right gel). The fluorescence signal remained unchanged after incubation for 60 min at 30 °C in the absence of SWI/SNF, but the addition of SWI/SNF and ATP led to the loss of ~60% of the Oregon green signal (Fig. 4a, left gel, lane 4). Loss of the Oregon green signal was also associated with the appearance of more quickly migrating, nonfluorescent MMTV DNA species (Fig. 4a, right gel, lane 4). These data are consistent with the ATP-dependent displacement of both histone H2A-H2B dimers, resulting in formation of tetrasome particles. Notably, the Swi2p-Arp7p-Arp9p subcomplex was unable to catalyze loss of the Oregon green fluorescence or to generate the more quickly migrating species, suggesting a defect in dimer displacement (Fig. 4a, left gel, lane 6). Likewise, a time course experiment showed that intact SWI/SNF displaced substantial amounts of H2A within 10 min of incubation, but the Swi2p-Arp7p-Arp9p subcomplex showed no activity in this assay (Fig. 4b).

To further investigate the ability of the Swi2p-Arp7p-Arp9p subcomplex to displace H2A-H2B dimers, we performed an *in vitro* chromatin immunoprecipitation (ChIP) analysis, using antibodies against H2A and H4 (ref. 19). In this assay, MMTV mononucleosomes were incubated with remodeling enzymes, proteins were cross-linked with formaldehyde, histone H2A or H4 was immunoprecipitated and the recovery of MMTV DNA was analyzed by PCR. Incubation with

(Fig. 4a, left gel) and ethidium bromide staining (Fig. 4a, right gel). The fluorescence signal remained unchanged after incubation for 60 min at 30 °C in the absence of SWI/SNF, but the addition of SWI/SNF and ATP led to the loss of ~60% of the Oregon green signal (Fig. 4a, left gel, lane 4). Loss of the Oregon green signal was also associated with the appearance of more quickly migrating, nonfluorescent MMTV DNA species (Fig. 4a, right gel, lane 4). These data are consistent with the ATP-dependent displacement of both histone H2A-H2B dimers, resulting in formation of tetrasome particles. Notably, the Swi2p-Arp7p-Arp9p subcomplex was unable to catalyze loss of the Oregon green fluorescence or to generate the more quickly migrating species, suggesting a defect in dimer displacement (Fig. 4a, left gel, lane 6). Likewise, a time course experiment showed that intact SWI/SNF displaced substantial amounts of H2A within 10 min of incubation, but the Swi2p-Arp7p-Arp9p subcomplex showed no activity in this assay (Fig. 4b).

To further investigate the ability of the Swi2p-Arp7p-Arp9p subcomplex to displace H2A-H2B dimers, we performed an *in vitro* chromatin immunoprecipitation (ChIP) analysis, using antibodies against H2A and H4 (ref. 19). In this assay, MMTV mononucleosomes were incubated with remodeling enzymes, proteins were cross-linked with formaldehyde, histone H2A or H4 was immunoprecipitated and the recovery of MMTV DNA was analyzed by PCR. Incubation with

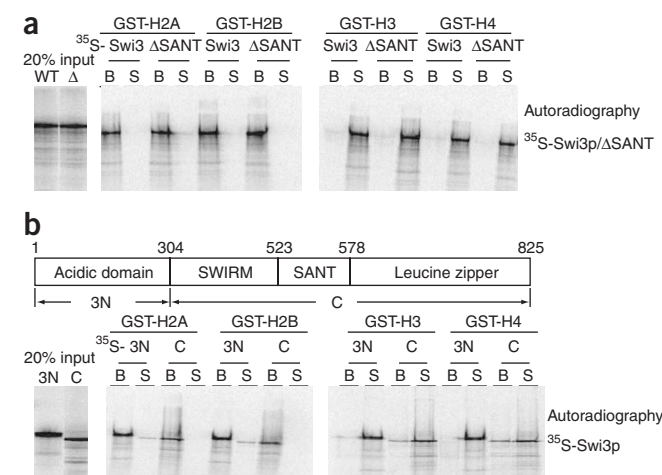
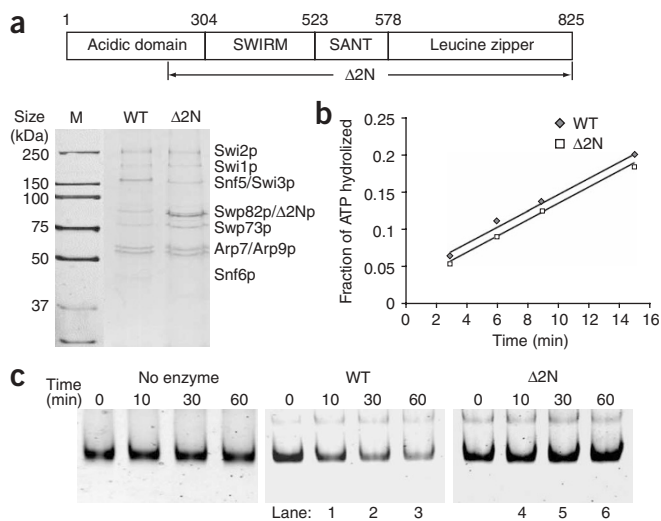


Figure 5 Swi3p has a novel histone-binding domain. (a) GST-histone tail fusion proteins were used in pull-down assays with *in vitro*-translated, <sup>35</sup>S-labeled full-length Swi3p and ΔSANT Swi3p. B, bound (100%); S, unbound supernatant (15%). (b) Top, schematic of Swi3p domains. Bottom, GST-histone tail pull-down assays with <sup>35</sup>S-labeled N-terminal domain of Swi3p (3N) or C-terminal domain (C).





**Figure 6** The acidic N-terminal domain of Swi3p is required for displacement of histone H2A. **(a)** Top, schematic of *swi3*- $\Delta$ 2N. Bottom, silver-stained gel of TAP-Swi2p preparations purified from wild-type or *swi3*- $\Delta$ 2N strains. M, molecular weight markers. **(b)** SWI/SNF- $\Delta$ 2N shows DNA-stimulated ATPase activity similar to that of intact SWI/SNF. ATPase assays were done as described in Methods. **(c)** SWI/SNF- $\Delta$ 2N is defective for displacement of Oregon green-labeled H2A from MMTV mononucleosomes. Reactions contained 30 nM fluorescent MMTV mononucleosome and 5 nM remodeling enzymes.

intact SWI/SNF led to the loss of  $\sim$ 60% of histone H2A in 30 min (Fig. 4c,d). As expected, SWI/SNF action had no effect on the levels of histone H4 associated with MMTV sequences. In contrast, only  $\sim$ 27% of H2A was displaced by the Swi2p–Arp7p–Arp9p subcomplex. Furthermore, addition of a two-fold greater amount of the Swi2p–Arp7p–Arp9p subcomplex led to only  $\sim$ 43% loss of H2A (Fig. 4d). Thus, in contrast to the equivalent activity of SWI/SNF and the Swi2p–Arp7p–Arp9p subcomplex in a variety of other remodeling assays, the minimal subcomplex is specifically defective in catalyzing the ATP-dependent displacement of histone H2A–H2B dimers.

### Swi3p contains a histone-binding domain

The inability of the Swi2p–Arp7p–Arp9p subcomplex to function efficiently in dimer-displacement assays suggested that dimer loss is not a simple consequence of ATP-dependent changes in histone–DNA interactions. Instead, these data suggest that dimer loss might involve interactions between histones H2A–H2B and SWI/SNF subunits other than Swi2p, Arp7p and Arp9p. One of the subunits missing from the minimal SWI/SNF complex is Swi3p, which has a 300-residue N-terminal domain that contains 25% acidic amino acid residues. A similar enrichment for acidic residues is a common feature of histone-binding proteins. To test whether Swi3p binds histones *in vitro*, we monitored the binding of  $^{35}$ S-labeled Swi3p to glutathione S-transferase (GST) fusion proteins that harbor the N-terminal domains of each of the four core histones. Notably, Swi3p was quantitatively retained on resins that harbored either GST–H2A or GST–H2B, but no binding to the GST–H3 or GST–H4 resins was observed (Fig. 5a). Likewise, 300 residues from the N-terminal domain of Swi3p were sufficient for GST–H2A and GST–H2B tail binding, and the C-terminal  $\sim$ 600 residues of Swi3p retained only weak binding activity (Fig. 5b). Thus, the N terminus of Swi3p seems to harbor a histone H2A–H2B-binding domain.

To test whether the N-terminal acidic domain of Swi3p is functionally relevant to SWI/SNF remodeling activities, we used TAP to purify SWI/SNF from a *swi3* mutant that encodes a truncated Swi3p with 200 residues deleted from the N terminus (*swi3*- $\Delta$ 2N). Notably, unlike for the *swi3*- $\Delta$ SANT allele, removal of the first 200 residues of Swi3p did not affect SWI/SNF assembly (Fig. 6a). The ATPase activity of the SWI/SNF- $\Delta$ 2N complex was equivalent to that of intact SWI/SNF (Fig. 6b), and both complexes functioned equivalently in the 601 mononucleosome restriction enzyme-accessibility assay (Supplementary Fig. 2 online). Thus, as expected from the analysis of the Swi2p–Arp7p–Arp9p subcomplex, the Swi3p N-terminal acidic domain is not required for ATPase or nucleosome-remodeling activity of SWI/SNF. We then tested the activity of SWI/SNF- $\Delta$ 2N for H2A–H2B dimer displacement, using the Oregon green–H2A fluorescence assay. Notably, the 200-residue deletion in the Swi3p acidic domain eliminated the ability of SWI/SNF to displace histone H2A, as monitored by loss of Oregon green fluorescence (Fig. 6c, compare lanes 1–3 with 4–6). Purified GST fusion protein harboring the 300-residue Swi3p acidic domain, when added to the reaction, was unable to rescue this defect in dimer loss *in trans* (data not shown). Likewise, addition of the Swi3p–Swp73p–Snf6p subcomplex to the Swi2p–Arp7p–Arp9p subcomplex did not reconstitute dimer-displacement activity (data not shown). These two subcomplexes do not stably interact *in vitro* (X.Y. and C.L.P., unpublished data), further suggesting that the Swi3p acidic domain functions most effectively when stably associated with SWI/SNF. These data indicate that the N terminus of Swi3p functions as a previously uncharacterized histone-interaction domain that is essential for histone H2A–H2B displacement *in vitro*.

### DISCUSSION

In several cases, the small,  $\sim$ 50-residue SANT domain that is found in many chromatin-regulatory proteins has key roles in functional interactions with the histone N-terminal tail domains<sup>30</sup>. In contrast, in the case of Swi3p, our data indicates that the SANT domain is crucial for SWI/SNF assembly. Likewise, one of the two SANT domains within the SMRT corepressor is also required for HDAC complex assembly<sup>38</sup>. Structural studies of the ISWI SANT domain confirm earlier predictions that this domain is composed of a bundle of three  $\alpha$ -helices, similar to the c-Myb DNA-binding domain<sup>39</sup>. A single-amino acid substitution or a small deletion in helix 3 of the Swi3p SANT domain yields *swi* or *snf* mutant phenotypes *in vivo*<sup>25</sup>, and both changes lead to SWI/SNF disassembly *in vitro*. Consistent with the observation that SANT deletions cause disassembly of SWI/SNF, we found that the 11-residue deletion in the Swi3p SANT domain leads to defects in the genome-wide gene expression profile that are similar to those resulting from a complete deletion of *SWI3* (X.Y. and C.L.P., unpublished data).

The purification of SWI/SNF from multiple *swi* or *snf* deletion strains or from the *swi3*- $\Delta$ SANT strain strongly supports a model in which SWI/SNF is composed of at least four interdependent modules (Fig. 7): (i) Swi2p–Arp7p–Arp9p, (ii) Swi3p–Swp73p–Snf6p, (iii) Snf5p and (iv) Swi1p. As inactivation of the Swp82p, Swp29p and Snf11p subunits does not lead to a loss of SWI/SNF function *in vivo*, the organization of these nonessential subunits has not been evaluated. The interdependent nature of the SWI/SNF subcomplexes is consistent with our previous gel-filtration analyses of crude yeast whole-cell extracts, where we found that loss of any one SWI/SNF subunit led to similar changes in the elution of the other subunits<sup>5</sup>. Furthermore, loss of the Swi3p subunit causes Snf6p to elute at an apparent monomer position<sup>5</sup>, consistent with our proposal of a Swi3p–Swp73p–Snf6p subcomplex. Notably, these subcomplexes confer

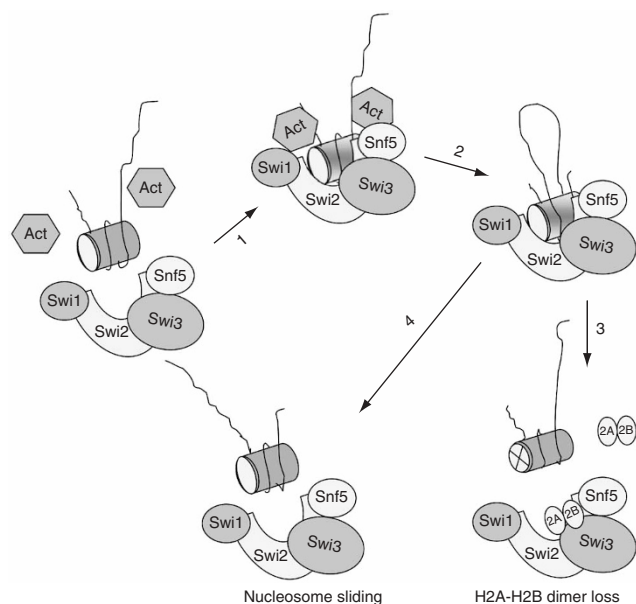


**Figure 7** A proposed model for SWI/SNF remodeling and functional organization. See text for details.

three distinct functions to the SWI/SNF complex (**Fig. 7**): the Swi2p–Arp7p–Arp9p subcomplex provides ATP-dependent DNA-translocation activity coupled to chromatin remodeling, the Swi3p–Swp73p–Snf6p subcomplex provides histone-binding activity coupled to dimer loss, and the Snf5p and Swi1p subunits provide gene-targeting functions by interaction with acidic activation domains of gene-specific activators<sup>11</sup>.

#### Function of a minimal Swi2p–Arp7p–Arp9p subcomplex

Previous studies have indicated that the isolated ATPase subunits of chromatin-remodeling enzymes are often sufficient to carry out much of the remodeling activity of the native, intact complex<sup>16,21,22</sup>. In the case of the human SWI/SNF complex, the BRG1 ATPase alone has ATPase activity and mononucleosome-remodeling activity that is ~20% that of the intact complex. Addition of the human homologs of the Snf5p (SNF5, or INI1) and Swi3p subunits (BAF155 and BAF170) is sufficient to restore full activity<sup>21,22</sup>. Likewise, for the yeast RSC complex, the isolated Sth1p ATPase is sufficient for ATP hydrolysis activity and DNA translocation<sup>16</sup>. In contrast, the catalytic subunit of the INO80 complex, Ino80p, is inactive by itself and requires the Arp5p and Arp8p subunits for ATPase activity and ATP-dependent nucleosome mobilization<sup>40</sup>. Likewise, the activities of the *Drosophila* and yeast ISWI ATPases are enhanced by the Acl1 (refs. 41,42) and Itc1 subunits<sup>43</sup>, respectively. For yeast SWI/SNF, we found that a Swi2p–Arp7p–Arp9p subcomplex is sufficient for ATP hydrolysis and for the majority of ATP-dependent chromatin-remodeling activities. As *ARP7* and *ARP9* are essential genes in yeast<sup>44</sup>, and as we have not been successful at expressing full-length Swi2p in bacteria or yeast cells, we have not been able to test whether Swi2p by itself is sufficient for these activities. We note, however, that the Arp7p and Arp9p subunits are also subunits of the RSC remodeling complex and that these subunits are not required for RSC assembly or remodeling activity<sup>45</sup>. Thus, it seems plausible that Arp7p and Arp9p may not have a role in remodeling per se but rather may stabilize the Swi2p ATPase.

#### The Swi3p N terminus contains a novel histone-binding domain

The ATP-dependent depletion of histone H2A–H2B dimers by chromatin-remodeling enzymes has been ascribed to these enzymes relatively recently, and consequently this activity has not previously been tested with isolated ATPase subunits. Our results indicate that ATP-dependent dimer loss is not efficiently catalyzed by the Swi2p–Arp7p–Arp9p ATPase subcomplex; the Swi3p subunit contributes an acidic histone-binding surface. Previous studies have shown that the yeast Nap1p histone chaperone can also promote H2A–H2B dimer loss in an ATP-independent reaction<sup>46</sup>, and, like Swi3p, yeast Nap1p also interacts with histone tail domains. Notably, interaction with histone tails is required for the nucleosome assembly activity of yeast Nap1p<sup>47</sup>. How interactions with the tail domains can facilitate nucleosome assembly or disassembly reactions is not yet clear.

It has been known for some time that the acidic N terminus of Swi3p is not a conserved feature of human Swi3p homologs BAF155 and BAF170, and thus the functional importance of this domain had not been tested. However, recently it was reported that the ATP-dependent dimer-displacement activity of the human SWI/SNF complex is stimulated by the acidic protein nucleolin<sup>48</sup>. These data suggest that human Swi3p homologs may not have conserved their acidic domains because SWI/SNF was able to take advantage of a functional interaction with other histone chaperones, such as nucleolin.

Our results indicate that the acidic N terminus of Swi3p is essential for ATP-dependent dimer loss *in vitro*; however, deletion of this acidic domain does not lead to obvious *swi* or *snf* mutant phenotypes *in vivo* (X.Y. and C.L.P., unpublished data). For instance, strains that harbor a *swi3* allele encoding a 300-residue N-terminal truncation of Swi3p grow at wild-type rates, and this change does not lead to defects in expression of two SWI/SNF-dependent target genes, *SUC2* and *HO-lacZ*. Although these results might suggest that ATP-dependent dimer loss does not contribute extensively to transcriptional control *in vivo*, we believe that it is more likely that this activity controls only a small subset of SWI/SNF-dependent genes. Consistent with this view, it is known that ATP-dependent dimer loss is highly DNA sequence dependent<sup>19</sup>, and thus it is expected that only a subset of remodeling events *in vivo* will displace dimers. Alternatively, it is possible that one or more abundant histone chaperones that are present within cells may compensate for the lack of the Swi3p N terminus.

#### Dimer loss versus DNA translocation

Recent data from both our lab and others support a DNA translocation model for ATP-dependent remodeling by the SWI/SNF family of enzymes<sup>15,16,49</sup>. In this model, SWI/SNF binds a single nucleosome in a substrate-binding pocket and interacts with nucleosomal DNA near the dyad axis<sup>4,16,17</sup> (**Fig. 7**, arrow 1). ATP-dependent DNA translocation generates a dynamic loop of DNA on the nucleosomal surface that has an average size of ~100 bp and rapidly dissipates by a continuous or discontinuous process<sup>15</sup> (**Fig. 7**, arrow 2). The formation of an intranucleosomal DNA loop probably reflects a transient intermediate in the process of nucleosome mobilization (**Fig. 7**, arrow 4). In addition, it seems likely that DNA loop formation may also be a prerequisite for displacement of histone H2A–H2B dimers, as loss of DNA–histone contacts is predicted to destabilize the histone dimers<sup>35,50</sup>, making them more prone to capture by histone-binding proteins such as the Swi3p acidic domain (**Fig. 7**, arrow 3). If this is the case, then it may explain why the Swi2p–Arp7p–Arp9p subcomplex retained some ability to displace H2A according to an *in vitro* ChIP assay, but this same subcomplex was inactive for H2A displacement in the Oregon green assay. The ChIP assay measures the ATP-dependent decrease in the ability to cross-link H2A to MMTV DNA,

and destabilization of the dimers owing to DNA translocation may lead to decreased cross-linking. In contrast, the Oregon green assay requires that the dimers be completely displaced from the MMTV mononucleosome. Thus, dimer displacement may involve at least two distinct steps: (i) destabilization of the H2A-H2B dimers owing to ATP-dependent intranucleosomal DNA loop formation, and (ii) H2A-H2B dimer capture by the Swi3p subunit.

## METHODS

**TAP-SWI/SNF purification.** Snf2p, Swi1p, Snf5p and Snf6p were C-terminally tagged with a protein A-calmodulin-binding domain TAP cassette at the endogenous locus of isogenic strains CY666 (wild-type), CY667 (*swi3Δ*) and CY669 (*swi3-ΔSANT*), as described<sup>51</sup> (see also ref. 4). SWI/SNF was purified as described<sup>4</sup>, with minor modifications (see **Supplementary Methods** online). The purity and components of each complex were confirmed by 8%–10% SDS-PAGE, followed by silver staining or western blotting. For mass spectrometry, individual bands were excised from the gel after silver staining. Remodeling enzyme concentrations were determined from a combination of western blots and ATPase activities.

**Histone protein purification and octamer reconstitution.** *Xenopus* histone H2A-S113C was generated by site-directed mutagenesis (Stratagene). All histone proteins were expressed, purified from inclusion bodies and reconstituted as octamers as described<sup>52</sup>.

**Reconstitution of nucleosomal array and mononucleosome.** 208-11 DNA templates were released from plasmid CP589 by NotI and HindIII restriction enzyme digestion and purified from agarose gel. The 601 DNA templates contain 343 bp of DNA released from plasmid CP1024 by EcoRI and HindIII restriction enzyme digestion. Mouse mammary tumor virus (MMTV) DNA template contains 350 bp of DNA with a centrally located nucleosome B positioning sequence and was purified after PCR amplification. 5S-208-11 and 601 templates were end labeled with [ $\alpha$ -<sup>32</sup>P]dCTP by Klenow fill-in at 37 °C and purified through a Sephadex G-25 column after phenol-chloroform extraction. Nucleosomal arrays and mononucleosomes were assembled by stepwise dialysis at 4 °C, using histone octamer/DNA ratios of 0.9–1.0 (ref. 53).

**ATPase activity and kinetics.** DNA-stimulated ATPase activity of each purified SWI/SNF complex was tested in a 10- $\mu$ l reaction mixture containing 20 mM Tris (pH 8.0), 5 mM MgCl<sub>2</sub>, 0.2 mM DTT, 5% (v/v) glycerol, 0.1% (v/v) Tween and 100  $\mu$ g ml<sup>-1</sup> BSA, with 1  $\mu$ g plasmid DNA, 100  $\mu$ M ATP, 0.01  $\mu$ Ci [ $\gamma$ -<sup>32</sup>P]ATP and 5 nM SWI/SNF<sup>53</sup>. Each reaction was incubated at 30 °C. Fraction of ATP hydrolyzed at each time point was quantified by ImageQuant version 1.2 (Amersham). For ATP hydrolysis kinetics, similar reactions were done in the presence of a series of different ATP concentrations varying from 3.125 to 1,000  $\mu$ M. Initial velocities were calculated from the slope of each linear plot of ATP hydrolysis by Microsoft Excel. Velocity was plotted as a function of ATP substrate concentration using KaleidaGraph version 3.6 (Synergy Software). Kinetic parameters were retrieved from nonlinear fitting to the Michaelis-Menten equation. Data from three independent experiments were averaged, and the s.d. was less than 15%.

**Remodeling assays.** Cruciform formation assays, and 601 mononucleosome accessibility and mobility assays was done as described<sup>32</sup>. Restriction enzyme-accessibility assays of 208-11-Sal arrays were done as described<sup>33</sup>.

**Histone H2A-H2B dimer-loss assay.** Reconstituted octamers containing H2A-S113C and H3-C110A were covalently labeled with Oregon green (Molecular Probes) fluorescent dye as described<sup>18</sup>. Free Oregon green dye was removed by 3 $\times$  dilution and concentration with a 10,000-MW Centricon concentrator (VIVA Life Science) in labeling buffer (10 mM Tris (pH 7.5), 2 M NaCl, 0.1 mM EDTA). H2A-H2B dimer-loss analysis was done in a 10- $\mu$ l reaction containing 30 nM MMTV mononucleosomes and 5 nM SWI/SNF in 5-50 buffer (10 mM Tris (pH 8.0), 50 mM NaCl, 5 mM MgCl<sub>2</sub>, 1 mM DTT, 0.1 mg ml<sup>-1</sup> BSA). Reactions were terminated by adding 2 $\times$  termination buffer containing 10% (v/v) glycerol and 200 ng competitor DNA to remove SWI/SNF, and quenched on ice for 30 min. Samples were resolved on 4% nondenaturing

polyacrylamide gels in 0.5 $\times$  TBE buffer (0.045 M Tris-borate (pH 8.3), 0.001 M EDTA). Oregon green signal was detected on a Kodak Imaging scanner with an excitation filter of 465 nm and an emission filter of 535 nm.

**MMTV mononucleosome reconstitution for *in vitro* ChIP assay.** Mononucleosome templates for the *in vitro* ChIP assay were generated with a 232-bp EcoRI-BamHI fragment containing the MMTV promoter sequence (from -221 to +1). The fragment was radiolabeled at the 5' ends with the Klenow fragment of DNA polymerase and [ $\alpha$ -<sup>32</sup>P]dCTP. Mononucleosomes were reconstituted by salt dialysis as described<sup>54</sup>, using recombinant *Xenopus* histones expressed in *Escherichia coli*<sup>52</sup>. Purification of the reconstituted material was done by glycerol-gradient ultracentrifugation using a linear gradient of 10%–30% (v/v) glycerol in 50 mM Tris-HCl (pH 8.0), 5 mM EDTA, 1 mM DTT and 0.1 mg ml<sup>-1</sup> BSA. Centrifugation was done in a Beckman SW60 rotor for 9 h at 55,000 r.p.m. and 4 °C. Fractions of 100  $\mu$ l were collected from the bottom of the gradient.

***In vitro* chromatin immunoprecipitation assays.** Nucleosome-remodeling reactions (10  $\mu$ l) were done in 10 mM HEPES (pH 7.9), 60 mM KCl, 6 mM MgCl<sub>2</sub>, 60  $\mu$ M EDTA, 2 mM DTT, 13% (v/v) glycerol containing 20 nM MMTV nucleosomes and 6 or 12 nM wild-type SWI/SNF or minimal SWI/SNF complex, in the presence of 1 mM ATP. Nucleosomes were incubated for 30 min at 30 °C, then for an additional 30 min with 250 ng of poly(dIdC) as competitor. Remodeled nucleosomes were cross-linked with 2.5% HCHO for 10 min at 37 °C, and the reaction was stopped by adding 0.1 M glycine (pH 7.5) for 5 min at room temperature. ChIP buffer (1 ml, containing 0.01% (w/v) SDS, 1.1% (v/v) Triton X-100, 1.2 mM EDTA, 16.7 mM Tris (pH 8.1), 167 mM NaCl, 1 mM PMSF, 1  $\mu$ g ml<sup>-1</sup> aprotinin and 1  $\mu$ g ml<sup>-1</sup> pepstatin A) was added and, after removal of an aliquot for input control (10% total volume), mononucleosomes were immunoprecipitated with antibodies against histone H2A or H4 (ref. 55). Before extraction with phenol-chloroform and ethanol precipitation, the samples were de-cross-linked at 65 °C. The PCRs were done with Taq DNA polymerase under standard conditions. The specific primers (sequences available on request) generate a 232-bp fragment of nucleosome B of the MMTV promoter. PCR products were resolved on 1% agarose gels and stained with ethidium bromide.

***In vitro* translation and GST pull-down assay.** PCR-amplified DNA fragments and pCMX vector were digested with XhoI and PstI and purified from agarose gel. The insert fragment was ligated into pCMX vector with T7 promoter. All constructs were confirmed by sequencing analysis. Full-length Swi3p and the N-terminal 300 amino acids of Swi3p were translated and labeled with <sup>35</sup>S-methionine using the TNT T7 coupled transcription-translation system *in vitro* (Promega).

GST or GST-histone N-terminal tail fusions were expressed and purified from *E. coli* as described<sup>56</sup> (see **Supplementary Methods** for minor modifications). For GST pull-down assay, 5  $\mu$ l of each *in vitro*-translated reaction was mixed with 20  $\mu$ l of 50% (v/v) GST slurry (as background control) or GST-histone tails. Each reaction was adjusted with binding buffer (20 mM Tris (pH 8.0), 150 mM NaCl, 0.25 mM EDTA, 1 mM DTT, 0.1% (v/v) Triton X-100, 0.1 mg ml<sup>-1</sup> BSA, 1 mM PMSF) to a final volume of 200  $\mu$ l. After incubation for 2 h at 4 °C, GST resins were recovered by centrifugation and 15% of the supernatant was removed for an unbound fraction. The resins were washed with 1 ml binding buffer three times and resuspended in 2 $\times$  SDS sample buffer as 'fraction bound'. Samples were resolved by 10% SDS PAGE and gels were dried and autoradiographed.

*Note: Supplementary information is available on the Nature Structural & Molecular Biology website.*

## ACKNOWLEDGMENTS

We thank J. Reese (Penn State University) for SWI/SNF antibodies used for western blotting, and T. Owen-Hughes (Dundee) for the gift of T4 endonuclease VII. This work was supported by a grant from the US National Institutes of Health to C.L.P.

## COMPETING INTERESTS STATEMENT

The authors declare no competing financial interests.



Published online at <http://www.nature.com/nsmb/>

Reprints and permissions information is available online at <http://npg.nature.com/reprintsandpermissions>

1. Jenuwein, T. & Allis, C.D. Translating the histone code. *Science* **293**, 1074–1080 (2001).
2. Peterson, C.L. & Laniel, M.A. Histones and histone modifications. *Curr. Biol.* **14**, R546–R551 (2004).
3. Smith, C.L. & Peterson, C.L. ATP-dependent chromatin remodeling. *Curr. Top. Dev. Biol.* **65**, 115–148 (2005).
4. Smith, C.L., Horowitz-Scherer, R., Flanagan, J.F., Woodcock, C.L. & Peterson, C.L. Structural analysis of the yeast SWI/SNF chromatin remodeling complex. *Nat. Struct. Mol. Biol.* **10**, 141–145 (2003).
5. Peterson, C.L., Dingwall, A. & Scott, M.P. Five SWI/SNF gene products are components of a large multi-subunit complex required for transcriptional enhancement. *Proc. Natl. Acad. Sci. USA* **91**, 2905–2908 (1994).
6. Cairns, B.R., Levinson, R.S., Yamamoto, K.R. & Kornberg, R.D. Essential role of Swp73p in the function of yeast Swi/Snf complex. *Genes Dev.* **10**, 2131–2144 (1996).
7. Cairns, B.R., Henry, N.L. & Kornberg, R.D. TFG3/TAF30/ANC1, a component of the yeast SWI/SNF complex that is similar to the leukemogenic proteins ENL and AF-9. *Mol. Cell. Biol.* **16**, 3308–3316 (1996).
8. Treich, I., Cairns, B.R., de los Santos, T., Brewster, E. & Carlson, M. SNF11, a new component of the yeast SNF-SWI complex that interacts with a conserved region of SNF2. *Mol. Cell. Biol.* **15**, 4240–4248 (1995).
9. Peterson, C.L., Zhao, Y. & Chait, B.T. Subunits of the yeast SWI/SNF complex are members of the actin-related protein (ARP) family. *J. Biol. Chem.* **273**, 23641–23644 (1998).
10. Peterson, C.L. & Tamkun, J.W. The SWI-SNF complex: a chromatin remodeling machine? *Trends Biochem. Sci.* **20**, 143–146 (1995).
11. Prochasson, P., Neely, K.E., Hassan, A.H., Li, B. & Workman, J.L. Targeting activity is required for SWI/SNF function in vivo and is accomplished through two partially redundant activator-interaction domains. *Mol. Cell* **12**, 983–990 (2003).
12. Cosma, M.P., Tanaka, T. & Nasmyth, K. Ordered recruitment of transcription and chromatin remodeling factors to a cell cycle- and developmentally regulated promoter. *Cell* **97**, 299–311 (1999).
13. Peterson, C.L. & Workman, J.L. Promoter targeting and chromatin remodeling by the SWI/SNF complex. *Curr. Opin. Genet. Dev.* **10**, 187–192 (2000).
14. Burns, L.G. & Peterson, C.L. The yeast SWI-SNF complex facilitates binding of a transcriptional activator to nucleosomal sites in vivo. *Mol. Cell. Biol.* **17**, 4811–4819 (1997).
15. Zhang, Y. *et al.* DNA translocation and loop formation mechanism of chromatin remodeling by SWI/SNF and RSC. *Mol. Cell* **24**, 559–568 (2006).
16. Saha, A., Wittmeyer, J. & Cairns, B.R. Chromatin remodeling through directional DNA translocation from an internal nucleosomal site. *Nat. Struct. Mol. Biol.* **12**, 747–755 (2005).
17. Zofall, M., Persinger, J., Kassabov, S.R. & Bartholomew, B. Chromatin remodeling by ISW2 and SWI/SNF requires DNA translocation inside the nucleosome. *Nat. Struct. Mol. Biol.* **13**, 339–346 (2006).
18. Bruno, M. *et al.* Histone H2A/H2B dimer exchange by ATP-dependent chromatin remodeling activities. *Mol. Cell* **12**, 1599–1606 (2003).
19. Vicent, G.P. *et al.* DNA instructed displacement of histones H2A and H2B at an inducible promoter. *Mol. Cell* **16**, 439–452 (2004).
20. Flaus, A., Martin, D.M., Barton, G.J. & Owen-Hughes, T. Identification of multiple distinct Snf2 subfamilies with conserved structural motifs. *Nucleic Acids Res.* **34**, 2887–2905 (2006).
21. Phelan, M.L., Schnitzler, G.R. & Kingston, R.E. Octamer transfer and creation of stably remodeled nucleosomes by human SWI-SNF and its isolated ATPases. *Mol. Cell. Biol.* **20**, 6380–6389 (2000).
22. Phelan, M.L., Sif, S., Narlikar, G.J. & Kingston, R.E. Reconstitution of a core chromatin remodeling complex from SWI/SNF subunits. *Mol. Cell* **3**, 247–253 (1999).
23. Peterson, C.L. & Herskowitz, I. Characterization of the yeast SWI1, SWI2, and SWI3 genes, which encode a global activator of transcription. *Cell* **68**, 573–583 (1992).
24. Wilson, B., Erdjument-Bromage, H., Tempst, P. & Cairns, B.R. The RSC chromatin remodeling complex bears an essential fungal-specific protein module with broad functional roles. *Genetics* **172**, 795–809 (2006).
25. Boyer, L.A. *et al.* Essential role for the SANT domain in the functioning of multiple chromatin remodeling enzymes. *Mol. Cell* **10**, 935–942 (2002).
26. Grant, P.A. *et al.* Yeast Gcn5 functions in two multisubunit complexes to acetylate nucleosomal histones: characterization of an Ada complex and the SAGA (Spt/Ada) complex. *Genes Dev.* **11**, 1640–1650 (1997).
27. Aasland, R., Stewart, A.F. & Gibson, T. The SANT domain: a putative DNA-binding domain in the SWI-SNF and ADA complexes, the transcriptional co-repressor N-CoR and TFIIB. *Trends Biochem. Sci.* **21**, 87–88 (1996).
28. Sterner, D.E., Wang, X., Bloom, M.H., Simon, G.M. & Berger, S.L. The SANT domain of Ada2 is required for normal acetylation of histones by the yeast SAGA complex. *J. Biol. Chem.* **277**, 8178–8186 (2002).
29. Yu, J., Li, Y., Ishizuka, T., Guenther, M.G. & Lazar, M.A.A. SANT motif in the SMRT corepressor interprets the histone code and promotes histone deacetylation. *EMBO J.* **22**, 3403–3410 (2003).
30. Boyer, L.A., Latek, R.R. & Peterson, C.L. The SANT domain: a unique histone-tail-binding module? *Nat. Rev. Mol. Cell Biol.* **5**, 158–163 (2004).
31. Havas, K. *et al.* Generation of superhelical torsion by ATP-dependent chromatin remodeling activities. *Cell* **103**, 1133–1142 (2000).
32. Smith, C.L. & Peterson, C.L. A conserved Swi2/Snf2 ATPase motif couples ATP hydrolysis to chromatin remodeling. *Mol. Cell. Biol.* **25**, 5880–5892 (2005).
33. Logie, C. & Peterson, C.L. Catalytic activity of the yeast SWI/SNF complex on reconstituted nucleosome arrays. *EMBO J.* **16**, 6772–6782 (1997).
34. Thastrom, A. *et al.* Sequence motifs and free energies of selected natural and non-natural nucleosome positioning DNA sequences. *J. Mol. Biol.* **288**, 213–229 (1999).
35. Kassabov, S.R., Zhang, B., Persinger, J. & Bartholomew, B. SWI/SNF unwraps, slides, and rewraps the nucleosome. *Mol. Cell* **11**, 391–403 (2003).
36. Shudrovsky, A., Smith, C.L., Lis, J.T., Peterson, C.L. & Wang, M.D. Probing SWI/SNF remodeling of the nucleosome by unzipping single DNA molecules. *Nat. Struct. Mol. Biol.* **13**, 549–554 (2006).
37. Flaus, A. & Owen-Hughes, T. Dynamic properties of nucleosomes during thermal and ATP-driven mobilization. *Mol. Cell. Biol.* **23**, 7767–7779 (2003).
38. Guenther, M.G., Barak, O. & Lazar, M.A. The SMRT and N-CoR corepressors are activating cofactors for histone deacetylase 3. *Mol. Cell. Biol.* **21**, 6091–6101 (2001).
39. Grune, T. *et al.* Crystal structure and functional analysis of a nucleosome recognition module of the remodeling factor ISWI. *Mol. Cell* **12**, 449–460 (2003).
40. Shen, X., Ranallo, R., Choi, E. & Wu, C. Involvement of actin-related proteins in ATP-dependent chromatin remodeling. *Mol. Cell* **12**, 147–155 (2003).
41. Ito, T. *et al.* ACF consists of two subunits, Acf1 and ISWI, that function cooperatively in the ATP-dependent catalysis of chromatin assembly. *Genes Dev.* **13**, 1529–1539 (1999).
42. Eberharter, A., Vetter, I., Ferreira, R. & Becker, P.B. ACF1 improves the effectiveness of nucleosome mobilization by ISWI through PHD-histone contacts. *EMBO J.* **23**, 4029–4039 (2004).
43. Gelbart, M.E., Rechsteiner, T., Richmond, T.J. & Tsukiyama, T. Interactions of Isw2 chromatin remodeling complex with nucleosomal arrays: analyses using recombinant yeast histones and immobilized templates. *Mol. Cell. Biol.* **21**, 2098–2106 (2001).
44. Cairns, B.R., Erdjument-Bromage, H., Tempst, P., Winston, F. & Kornberg, R.D. Two actin-related proteins are shared functional components of the chromatin-remodeling complexes RSC and SWI/SNF. *Mol. Cell* **2**, 639–651 (1998).
45. Szerlong, H., Saha, A. & Cairns, B.R. The nuclear actin-related proteins Arp7 and Arp9: a dimeric module that cooperates with architectural proteins for chromatin remodeling. *EMBO J.* **22**, 3175–3187 (2003).
46. Park, Y.J., Chodaparambil, J.V., Bao, Y., McBryant, S.J. & Luger, K. Nucleosome assembly protein 1 exchanges histone H2A–H2B dimers and assists nucleosome sliding. *J. Biol. Chem.* **280**, 1817–1825 (2005).
47. McQuibban, G.A., Comisso-Cappelli, C.N. & Lewis, P.N. Assembly, remodeling, and histone binding capabilities of yeast nucleosome assembly protein 1. *J. Biol. Chem.* **273**, 6582–6590 (1998).
48. Angelov, D. *et al.* Nucleolin is a histone chaperone with FACT-like activity and assists remodeling of nucleosomes. *EMBO J.* **25**, 1669–1679 (2006).
49. Jaskelioff, M., Gavin, I.M., Peterson, C.L. & Logie, C. SWI-SNF-mediated nucleosome remodeling: role of histone octamer mobility in the persistence of the remodeled state. *Mol. Cell. Biol.* **20**, 3058–3068 (2000).
50. Aoyagi, S. *et al.* Nucleosome remodeling by the human SWI/SNF complex requires transient global disruption of histone-DNA interactions. *Mol. Cell. Biol.* **22**, 3653–3662 (2002).
51. Tasto, J.J., Carnahan, R.H., McDonald, W.H. & Gould, K.L. Vectors and gene targeting modules for tandem affinity purification in *Schizosaccharomyces pombe*. *Yeast* **18**, 657–662 (2001).
52. Luger, K., Rechsteiner, T.J. & Richmond, T.J. Expression and purification of recombinant histones and nucleosome reconstitution. *Methods Mol. Biol.* **119**, 1–16 (1999).
53. Logie, C. & Peterson, C.L. Purification and biochemical properties of yeast SWI/SNF complex. *Methods Enzymol.* **304**, 726–741 (1999).
54. Vicent, G.P., Melia, M.J. & Beato, M. Asymmetric binding of histone H1 stabilizes MMTV nucleosomes and the interaction of progesterone receptor with the exposed HRE. *J. Mol. Biol.* **324**, 501–517 (2002).
55. Angelov, D. *et al.* Differential remodeling of the HIV-1 nucleosome upon transcription activators and SWI/SNF complex binding. *J. Mol. Biol.* **302**, 315–326 (2000).
56. Frangioni, J.V. & Neel, B.G. Solubilization and purification of enzymatically active glutathione S-transferase (pGEX) fusion proteins. *Anal. Biochem.* **210**, 179–187 (1993).